Synergistic effect of combined nanoparticles to elaborate exfoliated egg-white protein-based nanobiocomposites

Isabel Diañez, Inmaculada Martínez, Pedro Partal*

Dpto. Ingeniería Química, Centro de Investigación en Tecnología de Productos y Procesos Químicos (Pro^2TecS) – Campus de Excelencia Internacional Agroalimentario, ceiA3, Universidad de Huelva, Campus El Carmen, 21071 Huelva, Spain

*Corresponding author. Tel.: +34 959 21 99 97; Fax: +34 959 21 93 85

E-mail addresses: isabel.dianez@diq.uhu.es (I. Diañez), imgarcia@uhu.es (I. Martínez), partal@uhu.es (P. Partal)

ABSTRACT

Efficient dispersion of nanoclays in biopolymer matrices is a key problem in nanobiocomposite development. A particular challenge is the homogeneous dispersion of layered silicates, termed exfoliation in biopolymer matrices as opposed to agglomeration and intercalation of such filler materials, since inhomogeneous nanobiocomposites often have unsatisfying properties. This work reports the successful elaboration of egg white protein/montmorillonite clay nanobiocomposites obtained by thermomechanical processing. A synergistic effect of combined natural (MMT-Na) and organomodified (OMMT) nanoparticles has been observed to elaborate exfoliated egg-white protein-based nanobiocomposites. Tensile tests performed on the obtained nanobiocomposites showed that exfoliated nanobiocomposites display enhanced mechanical properties compared to those of the intercalated nanobiocomposites and neat matrix. These results clearly highlight the great interest in using combined nanoclays to obtain protein-based nanobiocomposites with improved properties.

KEYWORDS

A. Nano-structures; B. Thermomechanical; D. Electron microscopy; E. Compression moulding; Nanobiocomposite

1. INTRODUCTION

In the last few years, the development and use of biodegradable bioplastics has been attracting a great deal of research and industrial interest, as its properties are able to compete, in many cases, with those of the traditional petroleum-based plastics, while reducing the environmental pollution caused by plastic waste. In addition, bioplastics can be processed using conventional plastics machinery [1], and many of them are abundant and low-cost materials obtained from renewable sources [2], so that the replacement of synthetic polymers with biodegradable materials could be very beneficial not only from the environmental point of view, but also economically.

The main renewable sources of biopolymers are proteins, polysaccharides and lipids. Proteins are thermoplastic heteropolymers of both polar and non-polar amino acids that are able to form numerous intermolecular linkages, and undergo different interactions, yielding a wide range of functional properties [3]. As a case in point, ovalbumin, which is the major egg white protein and the only one containing free sulfhydryl buried in its core, can be denaturated by heating, making conversion of sulfhydryl groups into disulphide bonds takes place [4]. Thus, egg white proteins (albumen) is known to be a suitable raw material because of its desirable properties, such as high transparency, an improved mechanical behaviour and an easy processing by moulding, among other features, such as gelling or foaming. Because of this, albumen is a very common ingredient in food industry and bioplastics formulation, taking advantage of its wide variety of functional properties [5].

Because of these numerous benefits, the development and improvement of bioplastics is the aim of many research studies. In order to cover more demanding and specialized applications, enhanced and innovative features are needed, and a way to accomplish this is by adding certain types of nanoparticles to the polymer matrix, obtaining bio-based composite materials, also known as nanobiocomposites. These nanoaditives are often nanoclays, such as montmorillonites, that can be used either in their natural state or organically modified. These clays belong to the family of phyllosilicates, and are characterized by a layered structure: discs or platelets, with extension varying from 1 μm to 10 nm and a thickness of about 1 nm, which stack together, by Van der Waals forces, to form the primary particles of the material. In turn, these particles form aggregates whose size varies from 0.1 to 10 μm. A negative

charge inside the clay platelet is naturally counter-balanced by inorganic cations like Na^+, Li^+, Ca^{2+}, K^+ or Mg^{2+}, located into the inter-layer space. At this point, the clay is considered to be in its natural state. However, with the aim of obtaining more compatible formulations, a chemical modification of the clay is often carried out. This process is known as organo-modification. The most common technique of modifying nanoclays is the cationic exchange, which consists in the substitution of inorganic cations for organic ones (e.g. NH_4^+, MT2EtOH) [6].

Both affinity between components and processing conditions will determine the final morphology and behaviour of the composite material. When the interaction between the polymer and the clay is very poor, nanoparticles aggregates remain as such in the polymer matrix, no true nanocomposite is formed and mechanical properties are greatly affected compared to the original polymer. If moderate interaction is achieved, expansion of the clay interlayer occurs, due to the penetration of the polymer chains into the clay galleries, leading to an intercalated structure. When the original layered structure of the clay is lost during processing, clay platelets are dispersed into the continuous phase and there is obtained what is known as exfoliated structure, which is supposed to provide the greatest improvements in polymer performance [7]. This is due to the higher surface-to-volume ratio between the clay and the polymer matrix [8].

So far, most of improvements in bioplastics performance by addition of nanoclays are related to the enhancement of their barrier properties to gases and vapours [1], greater thermal stability [9] and better mechanical properties [10]. Nevertheless, in many cases, the attainment of higher values of Young's modulus and stress at break is accompanied by a decrease in elongation [8,11], a fact that could limit the use of these materials in some applications.

Up to now, in order to achieve the best possible distribution and performance of nanocomposites, three techniques have been mainly used: the in-situ polymerization, the solvent intercalation and the melt intercalation process [6]. However, the direct addition of nanoclays along with the other components, for obtaining nanocomposites by thermomechanical processing, could greatly facilitate the automation of the process and, therefore, its industrial application.

The aim of this work is to use the thermomechnical processing to incorporate both natural and modified montmorillonites (together and separately) into an albumen-based bioplastic matrix, and subsequently studying the morphology and thermomechanical behaviour of resultant biocomposites.

2. EXPERIMENTAL

2.1. Materials

The spray-dried egg white albumen (EW, with 80 wt. % protein, 8 wt. % moisture and 3 wt. % ashes) used was provided by OVOSEC S.A. (Spain). Glycerol, from Guinama (Spain), and distilled water were used as protein plasticizers. With regard to the nanoparticles, two selected montmorillonites from Southern Clay Products, Inc. (USA) were used: a) Cloisite® Na^+ (MMT-Na) (natural sodium); and b) Cloisite® 30B (OMMT) (methyl tallow (bis-2-hydroxy ethyl) quaternary ammonium modified montmorillonite).

2.2. Samples preparation

2.2.1. Samples formulation

Two different formulations, at 3 and 6 wt. % nanoclay, were prepared for each type: modified (OMMT) and non-modified (MMT-Na) clays. Additionally, the combination of both clays was also studied, at 3 wt. % of natural and 0.5 wt. % of organomodified montmorillonite content. In these formulations, a plasticizer/protein ratio of 0.4 was always maintained, where the plasticizer consisted of a blend of glycerol (G) and distilled water (W) at 50 wt. %. A "control" formulation, with no nanoclay, was also studied. The final overall compositions are included in Table 1.

Table 1. Final compositions of the samples studied.

Sample	Composition (wt. %)			
	W	G	EW	Clay
0-Clay	20.0	20.0	60.0	0.0
3-Clay	19.4	19.4	58.2	3.0
6-Clay	18.8	18.8	56.4	6.0
3-MMT-Na/0.5-	19.3	19.3	57.9	3.0/

OMMT				0.5

2.2.2. Thermoplastic processing

During the thermoplastic processing step, ingredients are mixed, for 10 min at room temperature, in the kneading tool (Rheomix 600p) of a torque-rheometer (Polylab, Thermo Haake GmbH, Germany) equipped with two counter-rotating rollers turning at 50 rpm [12]. This process can be considered adiabatic, since neither heating nor cooling was supplied to the kneading chamber. The values of both torque and temperature were continuously monitored and recorded throughout mixing process. Specific mechanical energy (SME) transferred to the material was then calculated from these torque data, by Eq. 1 [13]:

$$SME = \frac{\omega}{m}\int_0^{t_{mix}} M(t)\partial(t) \quad (1)$$

where ω (rad/s) is the mixing speed, m (g) is the sample mass, $M(t)$ (N·m) the torque and t_{mix} (s) the mixing time.

2.2.3. Compression moulding

Bioplastics were moulded by compressing the dough-like material resulting from the thermoplastic processing, at 120 ^{o}C and 100 bar gauge pressure, using different moulds to obtain two types of samples: according to ASTM D638 “Type IV” dogbone specimen dimensions for tensile tests, and 50x10x3 mm^3 rectangular specimens, for others. Bioplastics thus obtained were stored at 53% RH and room temperature.

2.3. Characterization

2.3.1. Dynamic mechanical thermal analysis (DMTA)

DMTA tests were performed with a Seiko DMS 6100 (Seiko Instruments, Japan), in double cantilever bending mode. Storage modulus E’ (elastic response) and loss modulus E” (viscous response) were determined by this technique as a function of temperature. From these data, the complex modulus (E*) was calculated as $|E^*|^2 = |E'|^2 + |E''|^2$. Temperature sweeps were carried out at a constant frequency of

1 Hz, being the applied strain always below 0.025% to assure that all tests were within linear viscoelasticity (LVE) region. A heating ramp of 2 ^{o}C/min was set between 30 and 170 ^{o}C.

2.3.2. Tensile tests

Tensile tests were carried out with a Shimadzu AG-IS testing machine at a single cycle of 50 mm/min, stretching to the breaking point to determine the Young's modulus and maximum stress and strain of the samples, meeting the ASTM D638-10 Standard Test Method for Tensile Properties of Plastics.

2.3.3. Water uptake

For each formulation, water absorption capacity was evaluated (after 2 and 48 h), gravimetrically, in samples immersed in 50 mL distilled water, at room temperature. Water absorption (Ab) was calculated as shown in Eq. 2:

$$Ab = \frac{W_1 - W_0 + W_{sol}}{W_0} \times 100 \quad (2)$$

where W_1, W_0 and W_{sol} are the weights of the wet specimen, specimen before swelling and water-soluble residue, respectively. All tests were done in triplicate.

2.3.4. X-ray diffraction (XRD)

X-ray diffraction assays were conducted in a Bruker D8 Advance X-Ray Diffractometer with a monochromatized CuKα radiation at 40 kV and 30 mA was used over a scanning range (2θ) from 2 to 30°, a step size of 0.05°, and a count time of 15 s per step. The clay gallery separation or d-spacing was calculated from Bragg's law using XRD results [14]:

$$d = \frac{n\lambda}{2sin\theta} \quad (3)$$

where d is the spacing between layers of the clay, n is a whole number, λ the wavelength of X-ray and θ the angle at the maximum point of the mean peak in the spectra.

2.3.5. Transmission electron microscopy (TEM)

Specimens for TEM observation were cut from nanobiocomposite blocks at room temperature, using a Leica EM UC7 Ultramicrotome, equipped with a glass knife, to obtain sections with thickness between 70 and 90 nm. Transmission electron images were taken with a Zeiss Libra 120 microscope, at an acceleration voltage of 80 kV.

2.3.6. Statistical analysis

The results obtained from the different measurements are reported as an average value of all replicates (at least, five replicates for tensile tests and three for others), more or less the standard deviation, as a measure of variability.

3. RESULTS AND DISCUSSION

3.1. Thermoplastic processing

The thermoplastic processing of bioplastics and biocomposites involves the intimate mixing of proteins, plasticizers and nanoclays, when appropriate. Figure 1 shows the evolution of torque and temperature during the mixing process.

The aim of this work is to develop a suitable processing method for the direct addition of nanoclays, by simply introducing them into the kneading chamber, together with the other components. This would be very advantageous for the applicability of nanobiocomposites, since it would not be necessary to add new stages in the process of industrial production, compared to that used for conventional plastics.

In all cases, torque values undergo a sharp initial rise between 0.0 and 2.5 min, as long. Nevertheless, some of the blends (6-MMT-Na and 3-MMT-Na/0.5-OMMT) show a slightly different behaviour to the others. Most of samples show an induction period, which occurs approximately during the first minute of mixing, but this effect disappears for the two aforementioned samples. During mixing of 0-Clay and 3-MMT-Na/0.5-OMMT, torque initially increases up to a maximum, after which it drops back to lower steady-state values. However, the time corresponding to the maximum torque (t_{Mmax}) decreases more clearly for 3-MMT-Na/0.5-OMMT, if compared to non-nanoreinforced bioplastic. The induction phase corresponds to the progressive formation of a dough-like material with viscoelastic properties from its

solid-liquid separate components, and its duration can be related to the compatibility and ease of constituents to interact, as well as wettability and diffusion characteristics [15].

3 wt %. nanoclay addition seems to cause a slight increment of torque values at the end of the mixing, being this effect more remarkable in the case of MMT- Na. However, this increment does not occur when 0.5 wt. % OMMT is added together with 3 wt. % MMT-Na.

In addition, as can be seen in Table 2, torque values undergo more increase at higher concentrations, probably due to the friction caused by the presence of a greater quantity of solid particles (6wt. %). Likewise, the higher solids content would be the responsible of the observed temperature increase, which never exceeded 55 ^{o}C.

Table 2. Specific mechanical energy (SME), maximum temperature (T_{max}), temperature increase (ΔT), maximum torque (M_{max}) and time corresponding to the maximum torque (t_{Mmax}) reached during thermoplastic processing.

Composition	SME (kJ/kg)	T_{max} (^{o}C)	ΔT (^{o}C)	M_{max} (N·m)	t_{Mmax} (min)
0-Clay	12.28	37.44	15.64	15.90	2.88
3-OMMT	14.73	41.34	17.09	17.89	2.50
6-OMMT	23.38	52.72	28.51	28.21	2.05
3-MMT-Na	15.85	42.78	21.03	20.81	10.00
6-MMT-Na	23.22	52.25	26.12	28.41	4.32
3-MMT-Na/0.5-OMMT	15.60	50.30	32.90	23.06	1.05

It is worth mentioning the case of 3-MMT-Na/0.5-OMMT. This system, despite its relatively low clay concentration, exhibits a temperature profile similar to those shown by the most concentrated systems. This mixing behaviour, showing the earliest torque peak, would point out enhanced interactions among bioplastic compound, mainly plasticizer/clay and protein. The presence of a small amount of more hydrophobic clay OMMT (in addition to the hydrophilic MMT-NA) seems to favours the interaction with

some hydrophobic protein fractions [16], leading to an improved dispersion of clay in the bioplastic matrix (as it will be confirmed later). As a result, the torque undergoes a quick increase (with no induction period) that overlaps with a fast temperature rise. Such a temperature evolution has been previously related to an exothermic protein chains reorganization due to shear and plasticizer interactions, which are more apparent as plasticizer/protein compatibility is higher (in this case, it would be enhanced by the blend of glycerol, MMT-NA and OMMT) [17].

Thermomechanical behaviour

The protein-based composite materials were subjected to dynamic temperature sweeps in bending mode, at temperatures between 30 and 175 ^{o}C (Figure 2).

Figure 2 shows the evolution with temperature of the complex modulus, which continuously decays as temperature increases. If compared to the neat matrix, the addition of 3 wt. % OMMT does not seem to have any effect on the thermo-mechanical behaviour of the bioplastic. On the contrary, the 3 wt. % EW/MMT-Na composite shows higher values of complex modulus than the neat matrix, being the module values higher for MMT-Na composites in the whole range of the temperature sweep. Slightly E* values are also observed if concentration is increased up to 6 wt. %. Nevertheless, the addition of both clays together seems to cause neither any change in complex modulus relative to the 3-MMT-Na samples.

In all cases, it can be seen what could be considered as a rubbery zone, approximately between 60 and 140 ^{o}C. However, this plateau zone becomes less evident with increasing the solids concentration, especially when it comes to MMT-Na or MMT-Na/OMMT biocomposites.

In addition, all the tanδ curves exhibit a first peak, at about 55 ^{o}C, corresponding to the gel-glasslike transition temperature (T_g) of the egg white protein [18].

At low temperatures (below 80 ^{o}C), the presence of solids limits the mobility of polymer chains. However, when the biocomposite undergoes a temperature increase, clay-matrix interactions are easier

to break than the interaction of the biopolymer with itself, which achieves a higher degree of entanglement without the addition of nanoclays, even compatible ones.

Furthermore, all the curves present a second peak, located at about 150 ^{o}C, most probably related to a thermal degradation of the material.

A less pronounced T_g peak, about 55 ^{o}C is observed for the bioplastics containing MMT-Na, which denotes that polymer chains mobility upon heating is more constrained by this type of nanoclay. This could be due to the hydrophilic character of Na-MMT, which might favour the establishment of hydrogen bonds with the plasticizer (water), this latter becoming less available for the plasticization of the protein matrix. A decrease in plasticizer content has already been found to increase cross-linking degree values [19]. On the contrary, above 80 ^{o}C, these samples present higher values of tanδ, if compared to their OMMT counterparts, probably due to the weakening of the coulombic interactions associated with the presence of cations Na^{+}, while EW/OMMT samples seem to be reinforced by heating and show a more elastic behaviour.

EW/MMT-Na/OMMT composites behave in a very similar manner to 3-MMT-Na samples up to approximately 120 ^{o}C but, at this point, at the beginning of the terminal region, combined-clays composites exhibit higher tanδ values, showing a more pronounced peak around 150 ^{o}C. In particular, by adding only 0.5 wt. % OMMT to 3 wt. % MMT-Na, tanδ grows to values of 6 wt. % samples.

These results suggest a higher degree of compatibility between the natural clay (MMT-Na) and the bioplastic at the lowest temperatures tested, if compared to the more hydrophobic organo-clay (OMMT), for which large clay aggregates are observed. Hence, OMMT seems to act like a filler, and its effect is only significant for the highest concentration studied (6 wt. %), except when added together with MMT-Na. On the contrary, MMT-Na most probably intercalates into the matrix, so that its modifying effect is notable even at the lowest concentration studied (3 wt. %), an effect which seems to intensify in the presence of OMMT, when compatibility between natural montmorillonite and polymer matrix seem to become even more pronounced.

3.2. Tensile properties

A representative tensile stress-strain response of each formulation studied can be seen in Figure 3.

Most of the specimens show a mostly plastic behaviour, with a small elastic range, this fact being more evident in the case of EW/OMMT samples, which could be considered as a perfectly plastic material, since the curve has almost zero slope within the plastic deformation region [20]. The rest of samples undergo a linear strain hardening until just before the failure of the material, but some differences can be seen. Both MMT-Na and MMT-Na/OMMT samples show a steeper strain hardening than non-nanoreinforced bioplastic, probably due to the hindrance to relative movement of polymer chains during stretching, caused by the presence of intercalated clay particles. Likewise, slightly higher values of ultimate stress are also achieved for these samples. However, as can be seen in Table 3, when referring to the elongation capacity, MMT-Na composites show the poorest behaviour, apart from OMMT samples, being MMT-Na/OMMT composites which elongate the most under tensile load.

Table 3. Mechanical properties of biocomposites, calculated from stress-strain curves of each sample.

Composition	Elastic moulus (MPa)	Tensile strength (MPa)	Strain at break (%)
0-Clay	83.6±8.2	7.2±0.9	113.3±16.9
3-OMMT	107.7±9.4	6.9±0.4	75.8±29.6
3-MMT-Na	121.0±8.8	8.3±0.7	79.7±20.0
3-MMT-Na/0.5-OMMT	84.6±5.5	7.3±0.7	91.3±31.1

Elongation capacity can also be considered a measure of compatibility and dispersion of nanoclays, since both aggregates and interphases between components with low affinity are potential break points when the material is under tensile load.

3.3. Water absorption capacity

Water absorption capacity of samples was determined, gravimetrically, with the aim of evaluating the effect of the different nanoclays and formulations. A reduction in the water uptake of samples may be,

besides an advantage in itself, an indication of a better dispersion of nanoparticles into the polymer matrix [21].

Table 4 presents the percentages of water absorbed, after 2 and 48 h, by the samples studied.

Table 4. Water absorption capacity (Ab) of samples, immersed in water at room temperature, after 2 and 48 h.

Composition	Ab (wt. %)	
	2h	48h
0-Clay	41.8±2.7	51.9±0.7
3-OMMT	41.7±3.0	48.2±0.9
6-OMMT	40.4±2.6	45.2±1.7
3-MMT-Na	38.0±0.1	50.4±0.4
6-MMT-Na	38.4±0.2	53.5±2.3
3-MMT-Na/0.5-OMMT	34.5±1.0	58.8±3.0

The addition of MMT-Na and OMMT to the egg white matrix is not seen to significantly reduce the water absorption, at the two immersion times studied, when added separately. Thus, the presence of OMMT has a larger effect after 48h. On the contrary, the degree of reduction in the water absorption of the samples containing MMT-Na was more significant after 2h. This fact could be due to the degree of dispersion of particles, but also to their nature. The greater dispersion, the more obstacles the water finds in its diffusion path, making it longer. This is usually known as the tortuous path effect [21], which could be the reason of reduction in short-time water uptake of MMT-Na samples. However, when it comes to OMMT, this reduction seems to be due rather to the hydrophobic character of this clay, which limits the amount of water that can accumulate in the biocomposite. Thus, although absorption is faster than in the case of MMT-Na nanobiocomposites, the final percentage is lower.

When added together, MMT-Na effect is accentuated in water absorption at 2h, due, probably, to the higher degree of dispersion favoured by the combination of both types of clay. However, after 48h of immersion, hydrophilic nature of MMT-Na seems to prevail, and water absorption increases for these samples.

3.4. Microstructural analysis

In order to determine the internal structure of the materials, samples were analysed by X-ray diffraction and transmission electron microscopy, so that assumptions derived from previous experimental results about compatibility and distribution of different nanoclays could be either confirmed or rejected.

Both nanoclays and bioplastics were subjected to XRD analysis, before and after the preparation of composites. Diffraction patterns of each sample are shown in Figure 4.

The presence of high-intensity peaks indicates a layered structure of the material, both in the presence and absence of nanoparticles. This fact could be in agreement with the existence of certain crystallinity of the bioplastic matrix, which determines the internal structure of the material. However, the peak corresponding to the control sample undergoes a shift when nanoclays are added, in some of the samples studied. In addition, both MMT-Na and OMMT particles original diffraction peaks disappear completely when introduced into the polymer matrix.

Samples containing 6 wt. % nanoclays show no shift of the mean diffraction peak when compared with non-reinforced bioplastic, and everything seems to indicate that the amount of solids is so high that their proper distribution within the polymer matrix is not possible, so nanoparticles remain forming agglomerates, which have no influence on material microstructure. However, when clay content is reduced to 3 wt. %, peaks shift to smaller angles, being this change more noticeable for MMT-Na nanobiocomposites. Since interlayer spacing (d_{001}) is inversely proportional to diffraction angle, peak shifting to lower angles indicates that this space is enlarged, as showed in Table 5.

Table 5. Mean diffraction peaks and interlayer spacing of biocomposites and clay particles.

Composition	2Θ (I_{max})	d_{001} (Å)

MMT-Na	7.55	11.70
OMMT	4.80	18.39
0-Clay	5.60	15.77
3-OMMT	5.55	15.91
6-OMMT	5.55	15.91
3-MMT-Na	5.60	15.77
6-MMT-Na	5.60	15.77
3-MMT-Na/0.5-OMMT	5.25	16.82

This effect is due to the introduction of polymer chains into the clay galleries, causing their expansion. This process leads to what is known as intercalated structure, and can be considered that a true nanobiocomposite has been formed, a fact that is reflected in the various improvements observed in samples performance along this work.

Nevertheless, the most interesting behaviour is that showed by the sample containing both types of nanoparticles. The diffraction pattern of the nanobiocomposite containing MMT-Na and OMMT has its main peak at a lower angle that all other samples (5.25^{o} against 5.55^{o} for its counterparts with the same clay content), what means that polymer chains have been able to penetrate and expand the interlaminar space of the clay even more than in the case of adding only MMT-Na. Moreover, the intensity of the main diffraction peak has significantly decreased for MMT-Na/OMMT nanobiocomposite, implying a greater degree of structural disorder. This fact could mean that some of the clay platelets have separated to the point that partial exfoliation has been achieved, what would be an explanation for the differences observed between MMT-Na and MMT-Na/OMMT samples.

A more intuitive information can be obtained from TEM images. Figure 5 shows an overall comparison of EW bioplastic and nanobiocomposites, at a medium magnification suitable for displaying a general view of the nanoparticles distribution within the biopolymer matrix. In these images, a clear difference among different samples can be seen. Figure 5.a presents a mainly homogeneous appearance,

corresponding to non-nanoreinforced egg white protein bioplastic, in which even the protein globular structure can be noticed, especially at the highest magnification studied. In the rest of images, the presence of nanoparticles gets evident. However, morphologies revealed in each case result significantly different. The most disparate structure is that showed by the organomodified montmorillonite composite (Fig. 5.c), which present large and stripe-shaped aggregates which also follow a defined orientation, arranged almost parallel to each other, what could be the reason for the poor mechanical response of these samples under tensile load. On the other hand, MMT-Na composites (Figs. 5.b and 5.d) present a more uniform distribution of nanoparticles, though indeed the addition of OMMT seems to have an important effect on the dispersion of clay platelets. Even though nanoparticles are well dispersed in both cases, the sample containing only MMT-Na presents thicker particles, what seem to be stacked nanoclay platelets, if compared with the MMT-Na/OMMT nanobiocomposite, in which these solid particles look considerably thinner and, in fact, showing what could be considered as an exfoliated structure.

This can be easily appreciated in Figure 6, where the higher magnification allows to notice the difference between the intercalation of MMT-Na platelets with the protein matrix and the almost complete exfoliation of clay layers, caused by the addition of OMMT.

4. CONCLUSIONS

Egg white protein/montmorillonite clay nanobiocomposites have been obtained by thermomechanical processing. The macromolecular structure of these egg white-based materials was affected by the nature of the nanoclays added. Moreover, the molecular/macromolecular compatibility between the clay layers and the egg white matrix, such the ability of both components to establish interactions, appeared as the key parameter governing the nanostructure, the mechanical properties and the water absorption capacity of resultant nanobiocomposites.

Although OMMT displayed a higher interlayer distance and a certain hydrophilicity brought by hydroxyl groups, it seemed that its hydrophobic character was preponderant, leading to a poor compatibility with the egg white matrix arising large clay aggregates and consequently worst tensile properties.

On the contrary, MMT-Na intercalates into the matrix, so that its modifying effect in thermomechanical properties is notable even at the lowest concentration studied (3 wt. %), an effect which seems to intensify in the presence of OMMT, when compatibility between natural montmorillonite and polymer matrix seem to become even more pronounced or synergic.

Based on X-ray diffractograms and TEM observations, a good dispersion/exfoliation of nanoclays was achieved, but the resulting tortuosity effect appeared not effective to significantly reduce the water absorption capacity although modified the kinetic of absorption.

ACKNOWLEDGEMENTS

This work is part of a research project sponsored by "Ministerio de Economía y Competitividad" (Ref. MAT2011-29275-C02-01). The authors gratefully acknowledge its financial support.

REFERENCES

1. Sanchez-Garcia MD, Lopez-Rubio A, Lagaron JM. Natural micro and nanobiocomposites with enhanced barrier properties and novel functionalities for food biopackaging applications. Trends Food Sci Technol 2010;21(11):528-536.

2. Darder M, Aranda P, Ruiz-Hitzky E. Bionanocomposites: A new concept of ecological, bioinspired, and functional hybrid materials. Adv Mater 2007;19(10):1309-1319.

3. Song Y, Zheng Q. Improved tensile strength of glycerol-plasticized gluten bioplastic containing hydrophobic liquids. Bioresour Technol 2008;99(16):7665-7671.

4. Fernandez-Espada L, Bengoechea C, Cordobes F, Guerrero A. Linear viscoelasticity characterization of egg albumen/glycerol blends with applications in material moulding processes. Food Bioprod Process 2013;91(C4):319-326.

5. Jerez A, Partal P, Martinez I, Gallegos C, Guerrero A. Egg white-based bioplastics developed by thermomechanical processing. J Food Eng 2007;82(4):608-617.

6. Pollet E, Avérous L. Recent Results in Nano-Biocomposites based on Montmorillonites. In: Vikas Mittal, editor. Advances in Polymer Nanocomposite Technology. New York: Nova Science Publishers, Inc, 2010. p. 315-354.

7. Chivrac F, Pollet E, Schmutz M, Avérous L. New Approach to Elaborate Exfoliated Starch-Based Nanobiocomposites. Biomacromolecules 2008;9(3):896-900.

8. Peelman N, Ragaert P, De Meulenaer B, Adons D, Peeters R, Cardon L, Van Impe F, Devlieghere F. Application of bioplastics for food packaging. Trends Food Sci Technol 2013;32(2):128-141.

9. Mohanty S, Nayak SK. Biodegradable Nanocomposites of Poly(butylene adipate-co-terephthalate) (PBAT) and Organically Modified Layered Silicates. J Polym Environ 2012;20(1):195-207.

10. Lee J, Kim KM. Characteristics of Soy Protein Isolate-Montmorillonite Composite Films. J Appl Polym Sci 2010;118(4):2257-2263.

11. Alboofetileh M, Rezaei M, Hosseini H, Abdollahi M. Effect of montmorillonite clay and biopolymer concentration on the physical and mechanical properties of alginate nanocomposite films. J Food Eng 2013;117(1):26-33.

12. Dealy JM. Rheometers for Molten Plastics. New York: Van Nostrand Reinhold, 1982. p. 255.

13. Redl A, Morel M, Bonicel J, Guilbert S, Vergnes B. Rheological properties of gluten plasticized with glycerol: dependence on temperature, glycerol content and mixing conditions. Rheol Acta 1999;38(4):311-320.

14. Claudio De Rosa FA. Methods in Crystal Structure Determination from X-Ray Diffraction. In: Claudio De Rosa FA, editor. Crystals and Crystallinity in Polymers. Hoboken: John Wiley & Sons, Inc., 2013. p. 123-184.

15. Pommet M, Redl A, Morel M, Guilbert S. A way to improve the water resistance of gluten-based biomaterials: Plasticization with fatty acids. Gluten Proteins 2004(295):439-442.

16. Lewis J, Snell N, Hirschmann D, Fraenkel-Conrat H. Amino Acid Composition of Egg Proteins. J Biol Chem 1950;186(1):23-35.

17. Gomez-Martinez D, Partal P, Martinez I, Gallegos C. Gluten-based bioplastics with modified controlled-release and hydrophilic properties. Ind Crop Prod 2013;43:704-710.

18. Gonzalez-Gutierrez J, Partal P, Garcia-Morales M, Gallegos C. Effect of processing on the viscoelastic, tensile and optical properties of albumen/starch-based bioplastics. Carbohydr Polym 2011;84(1):308-315.

19. Chevillard A, Angellier-Coussy H, Guillard V, Gontard N, Gastaldi E. Investigating the biodegradation pattern of an ecofriendly pesticide delivery system based on wheat gluten and organically modified montmorillonites. Polym Degrad Stab 2012;97(10):2060-2068.

20. Jones RM. Deformation Theory of Plasticity. Virginia: Bull Ridge Pub, 2009. p. 622.

21. LeBaron P, Wang Z, Pinnavaia T. Polymer-layered silicate nanocomposites: an overview. Appl Clay Sci 1999;15(1-2):11-29.

FIGURE CAPTIONS

Figure 1. Evolution with time of torque and temperature during thermoplastic processing of proteins, plasticizers and nanoparticles, at 50 rpm and room temperature.

Figure 2. DMTA test performed on the composite bioplastics, at 1 Hz in bending mode.

Figure 3. Stress-strain curves obtained from tensile tests carried out on ASTM D638 “Type IV” dogbone specimens, at 50 mm/min.

Figure 4. X-ray diffraction patterns of clays and biocomposites, at 40 kV and 30 mA.

Figure 5. TEM images of samples with (a) no nanoclay content, (b) 3 wt. % MMT-Na, (c) 3 wt. % OMMT and (d) a combination of 3 wt. % MMT-Na and 0.5 wt. % OMMT.

Figure 6. High-magnification TEM images, comparing 3 wt. % MMT-Na nanobiocomposites (a) with no addition of any other clay and (b) with the addition of a 0.5 wt. % OMMT.

Figure 1

Click here to download high resolution image

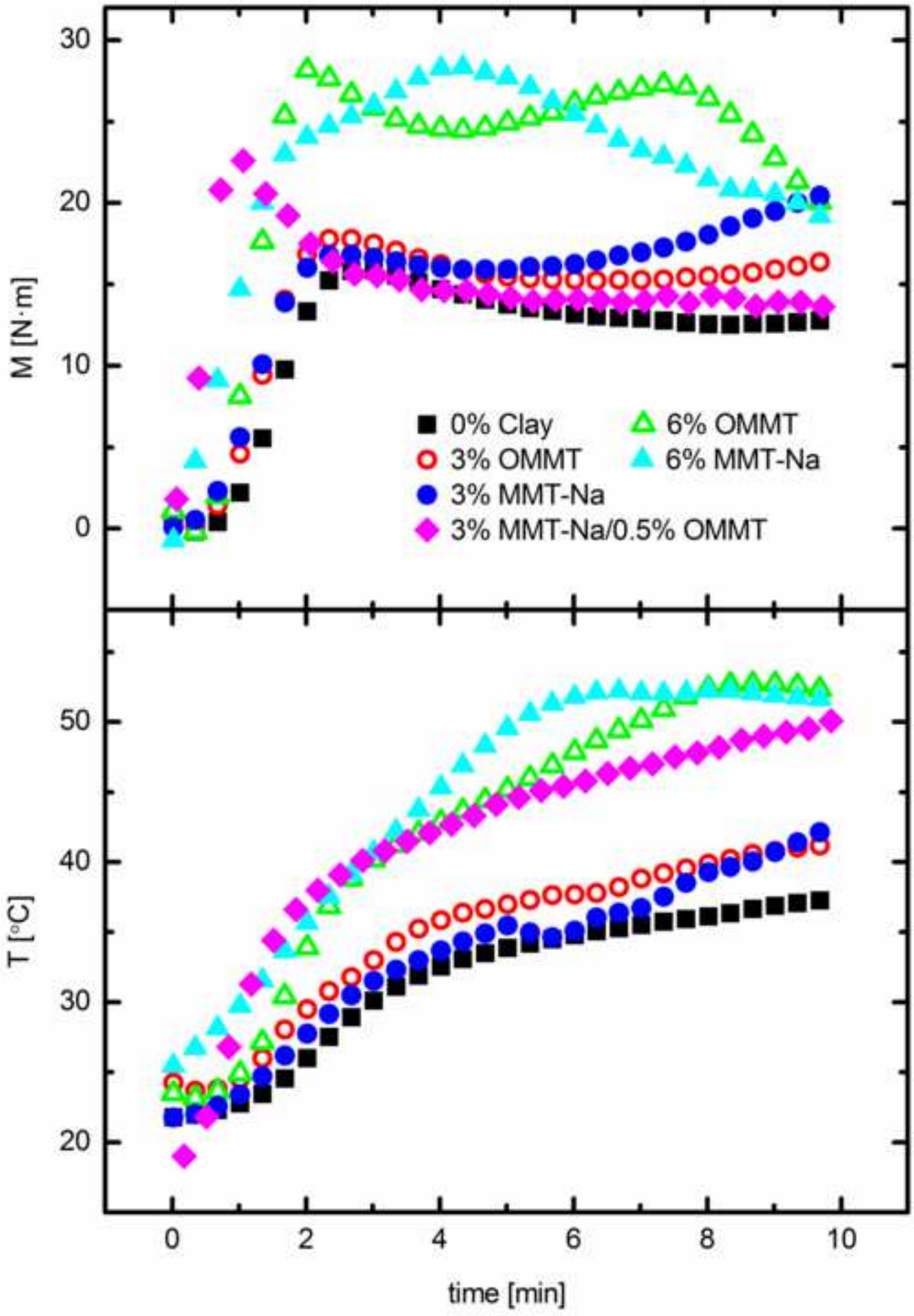

Figure 2

Click here to download high resolution image

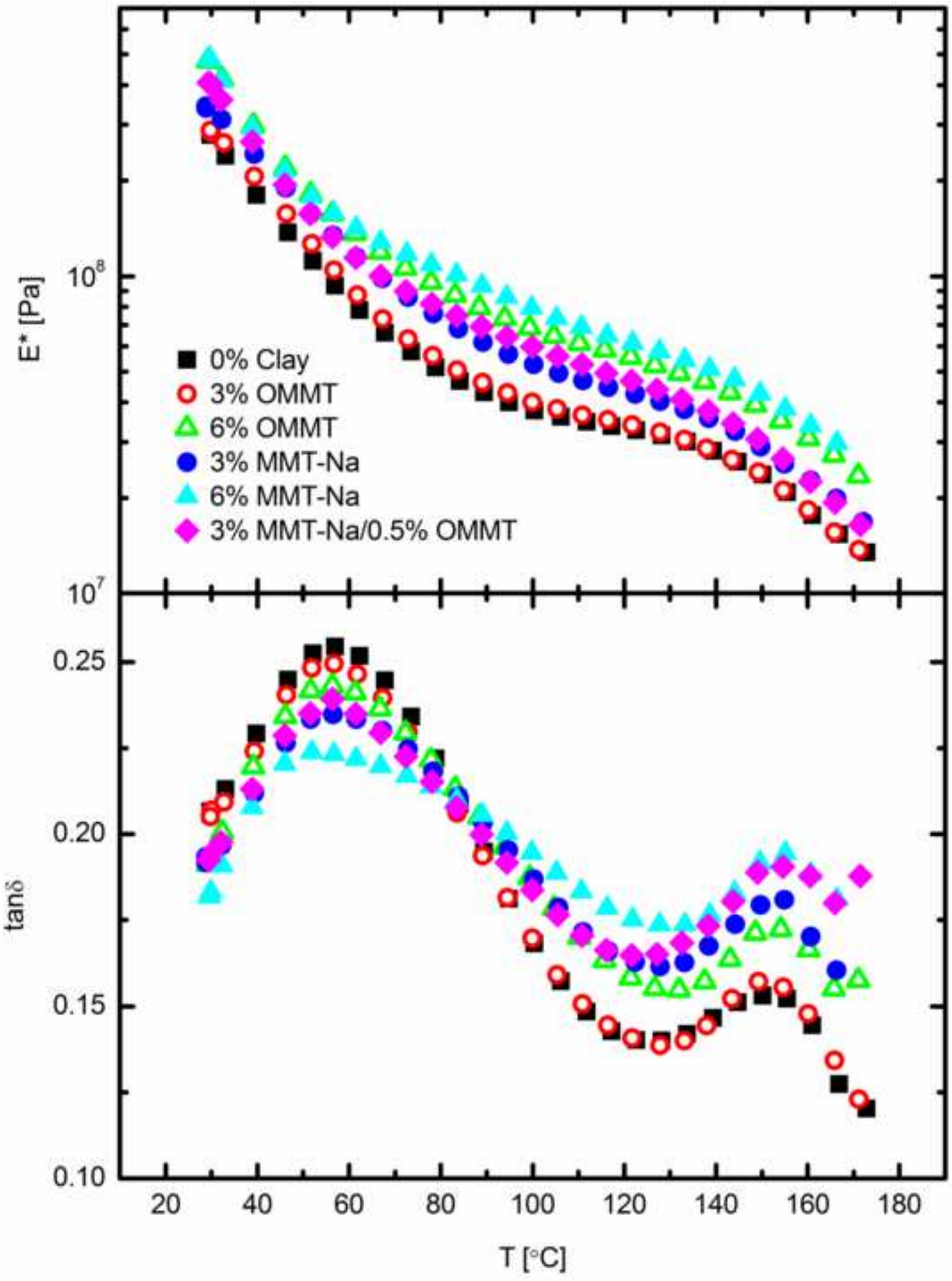

Figure 3

Click here to download high resolution image

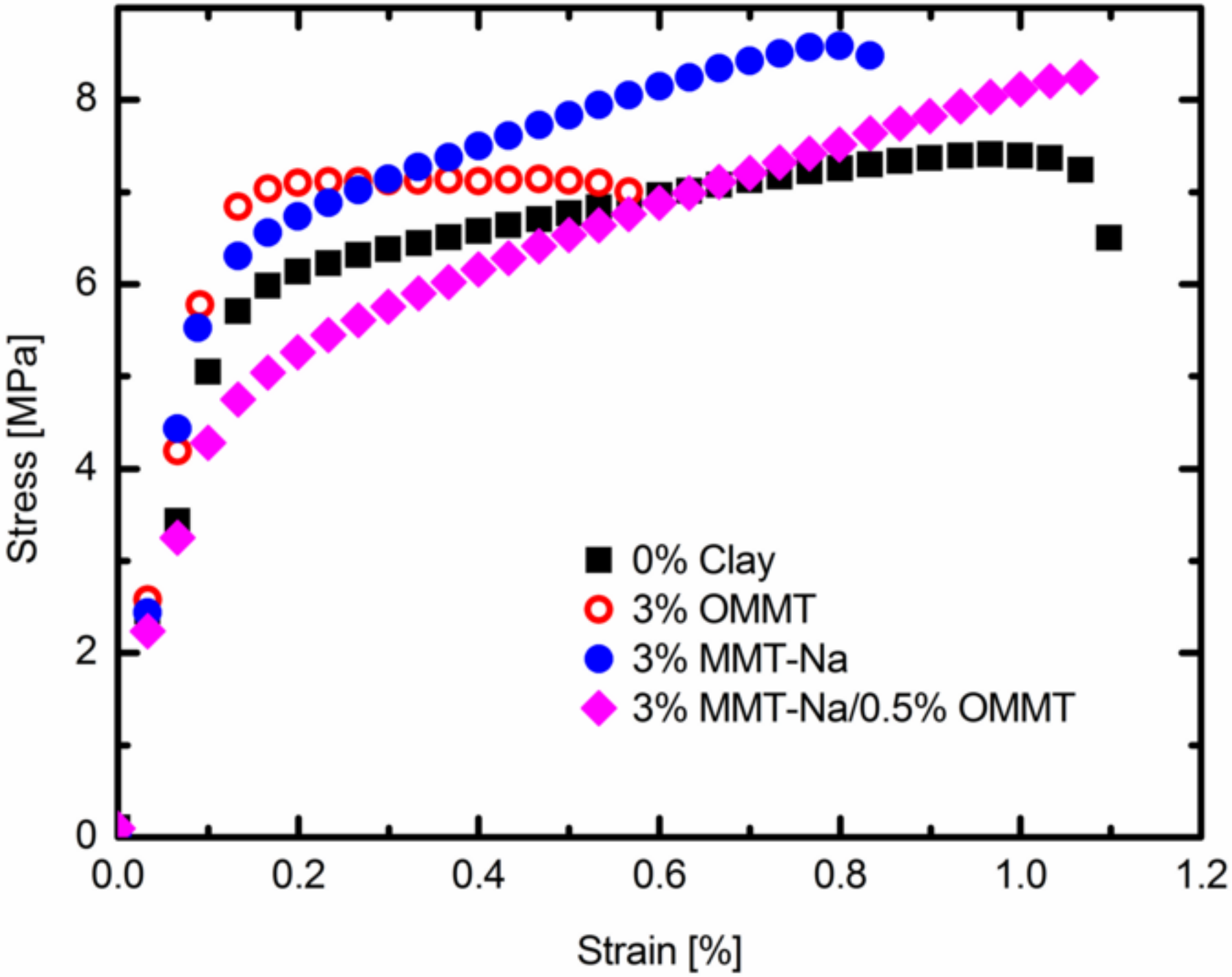

Figure 4

Click here to download high resolution image

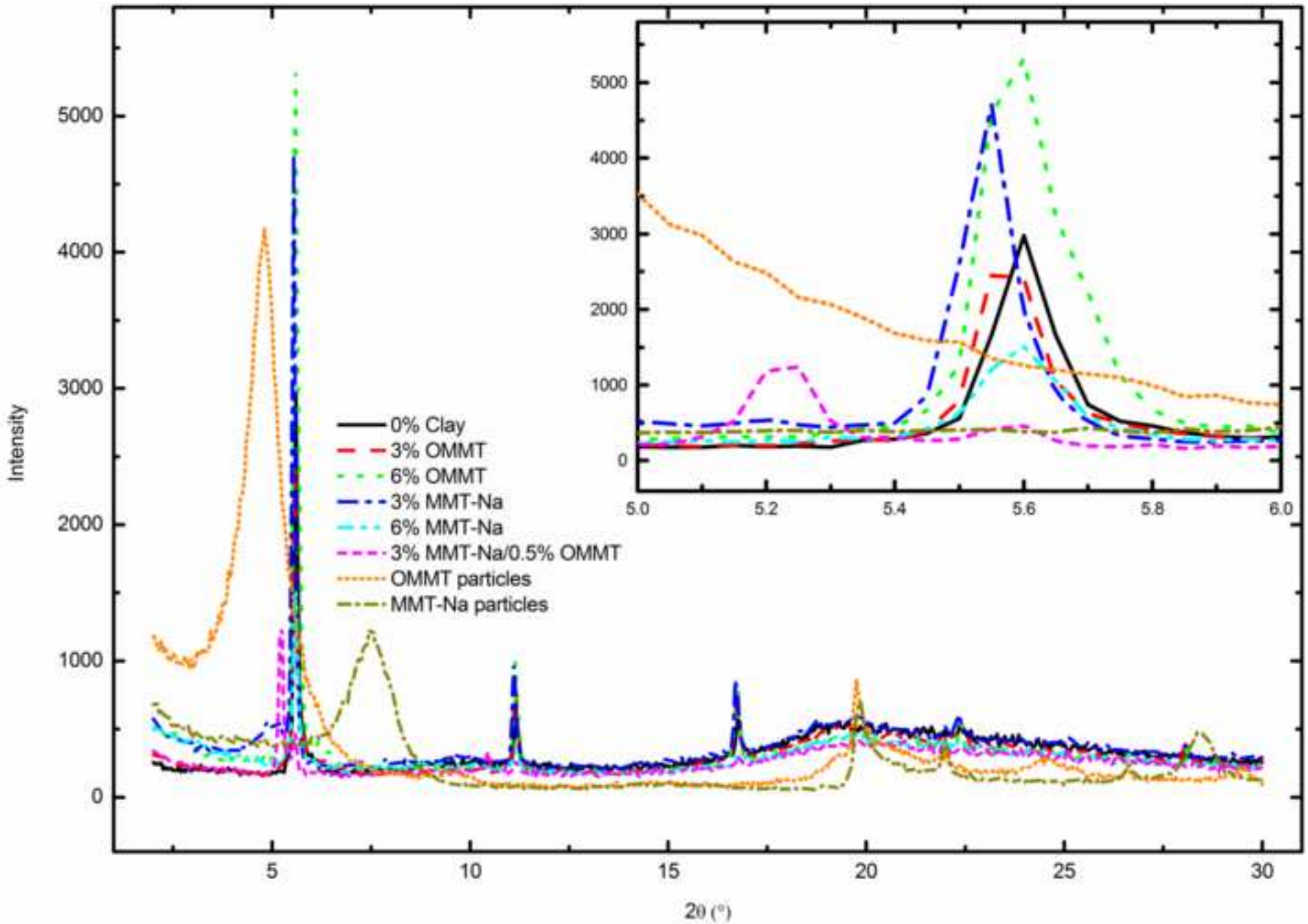

Figure 5

Click here to download high resolution image